SPECT and Planar Brain Imaging in Crack Abuse: Iodine-123-Iodoamphetamine Uptake and Localization

D.A. Weber, D. Franceschi, M. Ivanovic, H.L. Atkins, C. Cabahug, C.T.C. Wong and H. Susskind

Medical Department, Brookhaven National Laboratory, Upton, New York and Department of Radiology, Health Science Center, State University of New York, Stony Brook, New York

The uptake, distribution, and clearance properties of ^{123}I-IMP in the brain were evaluated in controls and asymptomatic crack users to investigate cerebral blood flow alterations in crack abuse. Serial dynamic planar images of the brain (0–25 min), SPECT of the brain (0.5 hr and 4 hr) and whole-body scans (75 min) were obtained in 21 crack abusers and 21 control subjects. Major observations include: (a) foci of abnormally reduced ^{123}I-IMP activity mainly in the frontal and parieto-occipital cortex or marked irregularities in the uptake of ^{123}I-IMP throughout the cerebral cortex consistent with moderate to severe disruption in regional cerebral blood flow were observed on the 0.5 hr SPECT images of 16/21 asymptomatic crack users; (b) no correlation could be demonstrated between the incidence or severity of SPECT perfusion abnormality with the frequency, amount or length of time of crack use; (c) focal perfusion defects observed in 6/21 crack users on the 0.5-hr SPECT images partially or completely filled-in on delayed SPECT at 4 hr in four of six subjects; (d) the rate of cerebral uptake of ^{123}I-IMP in crack users averaged 23% less than observed in control subjects over the first 25 min after tracer administration; and (e) ^{123}I-IMP activity reaching the brain of cigarette smoking control subjects (n = 14) at 25 min after injection averaged 42.5% less than in nonsmoking controls (n = 7). Quantitative measurements of the uptake and distribution properties of ^{123}I-IMP in the brain proved to be an objective, sensitive and useful measure of regional cerebral blood flow in crack abuse.

J Nucl Med 1993; 34:899–907

SPECT imaging of intravenously administered ^{123}I-labeled d,I-N-isopropyl-p-iodoamphetamine hydrochloride (IMP) provides a useful procedure to evaluate regional cerebral blood flow (rCBF) (*1*). The lipophilic radiopharmaceutical dissolves in the lipid membrane of the capillary vessels of the brain and passes through the blood-brain barrier by passive diffusion (*2*). Characterized by high and rapid first-pass extraction, the localization properties of ^{123}I-IMP provide an activity map of rCBF distribution in the brain (*1–5*). Retention in the brain is controlled by binding of ^{123}I-IMP to nonspecific amine binding sites and the washout of ^{123}I activity following its conversion to nonamphetamine metabolites. Washout and redistribution of the radiopharmaceutical is sufficiently slow to allow SPECT imaging of rCBF between 30 and 90 min after tracer administration. Its use and utility in providing a sensitive assay of cerebral perfusion in the workup of cerebrovascular disease, epilepsy and dementia is documented (*1*). The high sensitivity of the ^{123}I-IMP SPECT procedure to detect alterations in blood flow in the brain led us to use it to investigate possible alterations in rCBF caused by cocaine.

In preclinical ^{123}I-IMP SPECT studies of cerebral perfusion in the beagle dog, we observed that alterations in rCBF occur after acute doses of cocaine as low as 0.5 mg/kg (*6*). With crack users often using higher doses of cocaine (>2–4 mg/kg) three to four times per week, we thought that the SPECT brain perfusion procedure could offer a sensitive assay that might detect early alterations in rCBF in the asymptomatic crack subject before overt symptomatology or positive testing by other means. Despite increasing numbers of reports of neurovascular complications associated with crack abuse (*7–9*), very little information has been reported thus far on the use of nuclear medicine procedures to detect cerebral pathology in crack users (*10–12*). Our study was designed to investigate the use of ^{123}I-IMP SPECT imaging to detect alterations in rCBF in asymptomatic crack users.

MATERIALS AND METHODS

A total of 42 adult subjects participated in the study. These included 21 volunteers, control subjects and 21 subjects that had "snorted" or smoked crack, the cocaine alkaloid or free base, for 1–20 yr (Table 1). The studies were approved by the Institutional Review Committees at Brookhaven National Laboratory and the Health Sciences Center, State University of New York, Stony Brook. All subjects participating in the study were recruited using newspaper solicitation and informed consent was obtained. The control subjects presented without history of disorders or trauma affecting the central nervous system (CNS) or drug, including alcohol, abuse. Only asymptomatic crack users were accepted for study; those with history of other drug dependence were ex-

Received Nov. 10, 1992; revision accepted Feb. 11, 1993.
For correspondence or reprints contact: David A. Weber, PhD, Medical Department, Brookhaven National Laboratory, Upton, NY.

TABLE 1
Subject Data

	Sex		Age (yr)		Cigarette use			Crack use		
	M	F	Range	Mean	pk/d	pk/yr	Mean	g/wk	yr	last used
Controls(c)										
Nonsmokers(ns)	10	4	21–59	40	—	—	—	—	—	—
Smokers(s)	7	0	27–66	46	<1–2.5	8–31	19	—	—	—
Crack users(cr)										
Nonsmokers(ns)	5	0	23–50	32	—	—	—	3–13	3–19	1– 35 d
Smokers(s)	13	3	25–40	32	<1–2	1–44	16	2–15	1–20	1–240 d

cluded. Intravenous drug users were excluded to reduce the chance of including subjects with coexistent cerebral pathology resulting from AIDS or infection (*14*). Subjects with current or prior CNS disorders, head trauma or medication history for chronic conditions affecting cerebral metabolism or blood flow were excluded from the study. The sex, age, cigarette use and crack use history of the subjects are shown in Table 1.

All subjects had a series of imaging procedures following the intravenous administration of 111 MBq (3 mCi) of ^{123}I-IMP (SPECTamine, Iofetamine HCl ^{123}I Injection, MediPhysics, Paramus, NJ; studies were performed between 12/88 and 11/90). Subjects were instructed to rest with eyes open in a supine position in a quiet, dimly lit imaging room for at least 10 min before, during and 10 min after tracer administration. The rate of uptake and the localization properties of ^{123}I-IMP in the brain were evaluated from sequential dynamic images of a posterior view of the head acquired over the first 25 min following radiopharmaceutical administration and two SPECT procedures of the brain at 0.5 hr and 4 hr after ^{123}I-IMP administration. SPECT studies were collected as 60 projections, 40 sec per projection with a 1.5 zoom, using an elliptical orbit with a radius of rotation ranging from 11 to 14 cm. The 30-min SPECT study was used to assess regional cerebral perfusion. Delayed SPECT was used to evaluate redistribution and washout of tracer. Distribution properties of the radiopharmaceutical were investigated on anterior and posterior whole-body scans obtained at 75 min after radiopharmaceutical administration.

All imaging procedures were made on rotating gamma camera SPECT-imaging systems (Toshiba GCA-901A or Toshiba GCA-901SA, 38 cm × 50.8 cm UFOV). An ^{123}I parallel-hole collimator with a measured system spatial resolution of 9.5 mm (FWHM) at 10 cm depth with water as the scattering material (8.7 mm in air) was used to acquire images on the 901A system and an LEGP collimator (60-180 keV) with a measured system spatial resolution of 12.5 mm (FWHM) at 10 cm depth with water as the scattering material (10.2 mm in air) was used on the 901SA system. The reconstructed system axial spatial resolution for ^{123}I on the respective systems ranges from 8.5 and 10.1 mm at the periphery to 12.0 and 14.5 mm at the center for line source measurements in a 22-cm diameter water-filled phantom.

Image Processing and Data Analysis

Serial Dynamic Images. The rate of uptake of ^{123}I-IMP in the brain was determined in each subject from the time-activity curve obtained using a single region of interest (ROI) over both cerebral hemispheres on the dynamic image data collected over the first 25 min. The curve of the counting data was fit to a two-compartment uptake curve, $y(t) = \gamma - \alpha_1 e^{-\lambda_1 t} - \alpha_2 e^{-\lambda_2 t}$, using a least-squares fitting routine (Fig. 1). The biologic half-times, T_1 and T_2, of the two compartment curves and the time to 50% and 90%, T_{50} and T_{90}, of the maximum count rate in the cerebral hemispheres over the first 25 min after injection were determined.

SPECT. SPECT projections of the brain were preprocessed with a high-count flood source uniformity correction (120×10^6 counts) and a weighted 3 × 3 pixel smoothing routine. Tomographic slices (5.3 mm thick) were reconstructed using the conventional filtered backprojection method with a Shepp-Logan filter. Slices parallel to the canthomeatal line were reconstructed from the vertex to the base of the cerebellum using the first-order Chang attenuation correction method (*15*) with an experimentally determined attenuation coefficient of 0.135 cm^{-1} (*16*).

The regional distribution properties of ^{123}I-IMP in the brain were evaluated by visual inspection and quantitatively by using ROIs to obtain count (activity) information on 2-pixel (10.6-mm) thick tomographic slices. Transverse, sagittal and coronal tomographic slices were reconstructed on all SPECT studies. Transverse slices were inspected for abnormalities and sagittal and coronal views were reviewed for confirmatory evidence. Four reviewers (H.A., C.C., D.F., D.A.W.) read all studies in random order at the completion of the study. Final interpretations were based on a consensus agreement of all reviewers. For the quantitative evaluation, one to six ROIs were defined over each of nine cerebral structures on the tomographic slices. Forty ROIs were positioned over the temporal, frontal, parietal, prefrontal and visual cortex, basal ganglia, thalamus and cerebellum. ROI sizes ranged from 8 to 39 pixels. Positioning of the ROIs was adjusted for individual subjects; however, ROI size was held constant for all subjects. Figure 1 shows examples of ROI selection for two slices of the brain. In control subjects, typical count densities ranged from 150 to 200 counts/pixel/111 MBq (3 mCi) administered activity in the selected ROIs. The ratios of counts (activity) for contralateral regions, for regions to cerebellum and for the same regions, 4 hr/0.5 hr, were calculated.

Whole-Body Scans. Activity in selected organs was calculated as a percentage of retained dose from the geometric means of ROIs placed over selected organs divided by the geometric mean of ROIs of the whole body.

Statistics. The statistical significance of differences in ^{123}I-IMP uptake kinetics and distribution properties for control subjects and crack users was determined by applying the paired and unpaired Student's t-test. Statistical significance was selected as $p < 0.05$.

RESULTS

Rate of Uptake

The time-activity curves for ^{123}I-IMP uptake in the brain showed significant differences in the rates of uptake be-

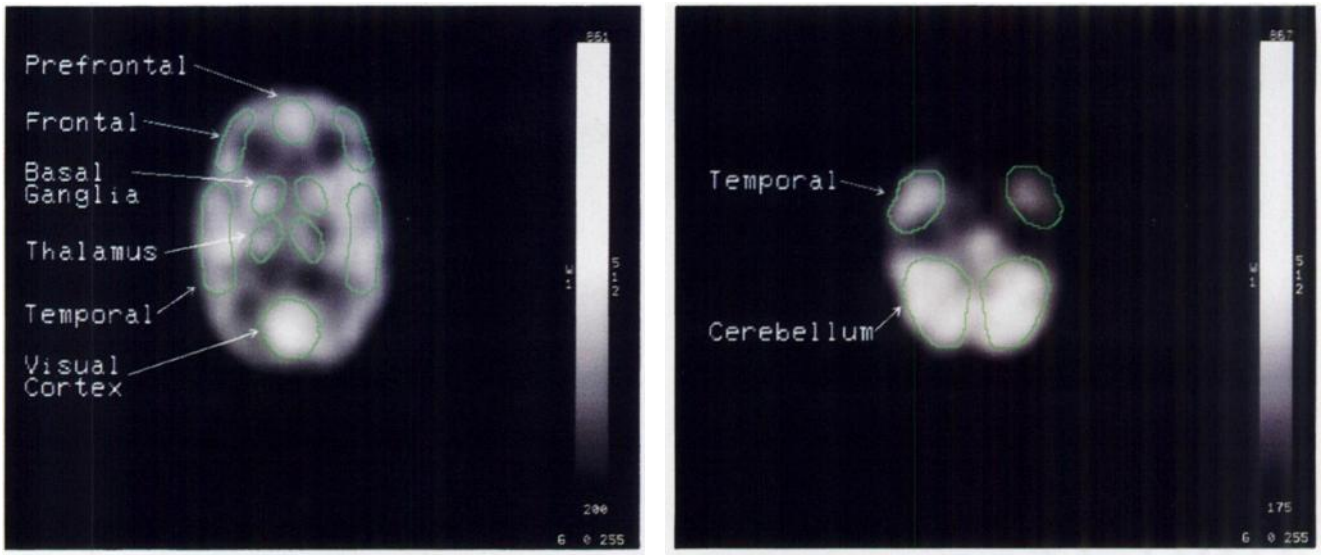

FIGURE 1. Example of ROI selection and positioning on two of six transverse slices of the brain used to analyze distribution properties of ^{123}I-IMP in the brain.

tween the crack users and the control subjects (Fig. 2, Table 2). The results showed a mean biological uptake half-time of T_2 = 419 ± 41 sec and T_{90} = 1005 ± 92 sec in 21 crack users as compared to T_2 = 340 ± 22 sec (p = 0.001) and T_{90} = 806 ± 220 sec (p = 0.0003) in 21 control subjects (Table 2). Smoking also influenced the rate of cerebral uptake. The mean biological uptake half-time of ^{123}I-IMP in the brain of nonsmoking crack users (T_2(ns-cr) = 391 ± 35 sec, n = 5) and smoking crack users (T_2(s-cr) = 432 ± 38 sec, n = 16) averaged 13% and 32% less than in the respective nonsmoking control (T_2(ns-c) = 345 ± 22 sec, n = 14, p = 0.03) and smoking control subjects (T_2(s-c) = 328 ± 50 sec, n = 7, p = 0.009). Smoking in the control population also significantly reduced the level of activity reaching the brain. The uptake plateau of ^{123}I-IMP activity in the brain of smoking control subjects (γ = 2.3 ± 0.8 c/mCi/s/100 p, n = 15) was 42.5% less than that observed in nonsmoking control subjects (γ = 4.0 ± 1.4 c/mCi/s/100 p, n = 7). The total counts in the SPECT projections collected for the 30-min SPECT studies of the four different patient groups were consistent with these findings.

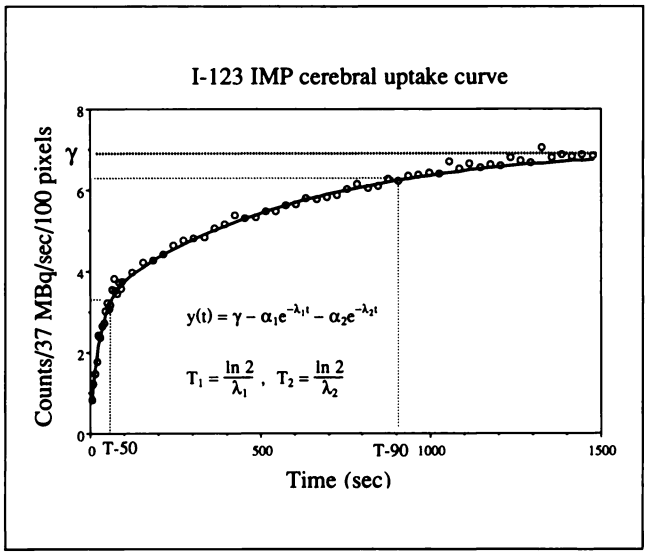

FIGURE 2. Time-activity curve for ^{123}I-IMP uptake in the brain of control subjects obtained from serial dynamic images of the brain recorded over the first 25 min following radiopharmaceutical administration. Rate of uptake is characterized by biologic half-times T1 and T2 and the time for activity to reach 50% (T_{50}) and 90% (T_{90}) of the uptake plateau seen within 25 min following ^{123}I-IMP administration.

Imaging Properties

The activity distribution of ^{123}I-IMP in reconstructed transverse slices from the SPECT studies was evaluated qualitatively by visual inspection and quantitatively by ROI analyses.

Visual Inspection

SPECT studies in the 21 asymptomatic crack users revealed three types of image findings. Normal perfusion images with good definition of cortical, subcortical and cerebellar structures were observed in 5/21 subjects; focal perfusion defects corresponding to regions of reduced blood flow were observed in 6/21 subjects, with 4/6 showing partial or complete filling in of the perfusion defect on delayed SPECT at 4 hr; and irregular decreases in tracer uptake, characterized by a loss of contrast and definition of ^{123}I-IMP uptake in the gray matter structures, were observed in 10/21 subjects (Figs. 3–5). In the last group, the severity of change was graded between 1 and 4, with 1 showing minimal loss in definition and mild asymmetries, ranging to 4 and showing poor definition of the cerebral cortex with decreased and highly variable or mottled uptake throughout the cortex. Image quality was typically very poor in the subjects interpreted as having mottled uptake with a grade of 3 or 4. Six of the subjects in the latter group were interpreted as having small to moderate changes (grades 1 or 2) and four subjects were read to have

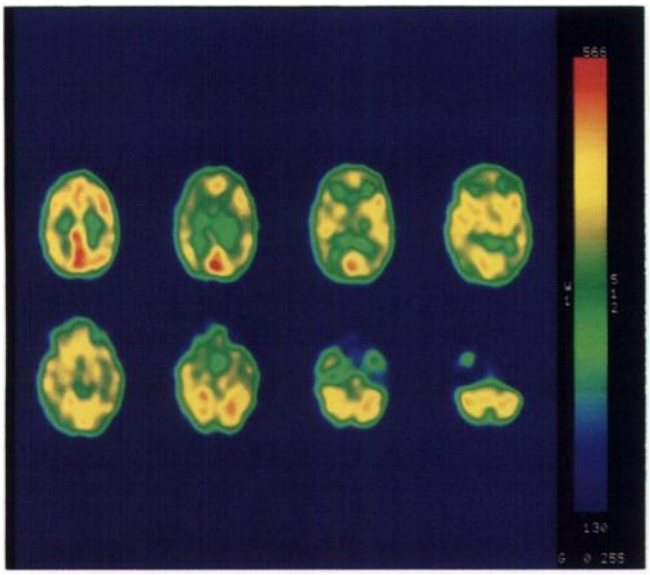

FIGURE 3. Two pixels (10.6 mm thick) transaxial SPECT slices of the brain from a control subject. Images show normal perfusion pattern with good definition of cortical, subcortical and cerebellar structures.

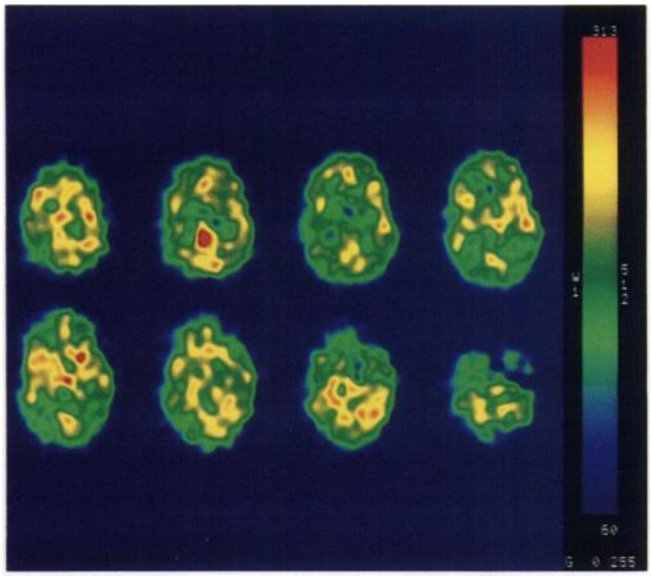

FIGURE 5. Transaxial SPECT slices (10.6 mm thick) of the brain from a crack user show marked irregularities in tracer uptake and loss of definition of the normal perfusion pattern in the cortical and subcortical structures and cerebellum. This image set was read as showing mottled uptake with a grade of 4.

highly irregular to major disorganization of ^{123}I-IMP uptake (grades 3 or 4) in the cortex.

No perfusion defects were seen in the SPECT studies in the 21 control subjects. Fifteen subjects had normal perfusion images and six subjects showed varying degrees of loss of definition and irregular uptake in cortical structures. Five subjects showed small to moderate changes (grades 1 and 2) and one subject showed greater irregularities and mottled uptake (grade 3).

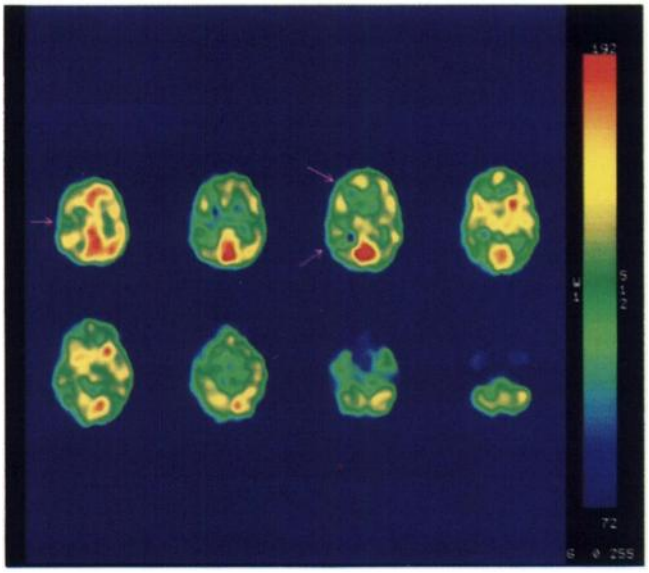

FIGURE 4. Transaxial SPECT slices (10.6 mm thick) of the brain from a crack user show focal defects in the right frontal cortex and in the right parieto-occipital region which correspond to regions of reduced blood supply.

Quantitative Regional Distribution Properties

The distribution properties of ^{123}I-IMP in the brains of controls and crack users were evaluated in terms of contralateral (left/right), region-to-cerebellum and regional retention (240 min/30 min) activity uptake ratios. The mean activity ratios for 15 contralateral ROIs in the frontal, parietal, temporal, thalamic, basal ganglia and cerebellar regions in controls and crack users were uniformly close to 1.0. No significant quantitative differences ($p > 0.05$) in uptake ratios were seen between the control and crack user groups. In comparison, small but statistically significant differences in contralateral uptake ratios were seen in the subjects interpreted to have perfusion defects (Table 3). The mean cerebellar uptake ratios for 24 regions-to-cerebellum, consisting of 9 unpaired regions in the prefrontal and visual cortex and 15 regions on the left for the frontal, parietal and temporal cortex, thalamus, basal ganglia and cerebellum showed variations in regional uptake in gray matter structures, however, these differences tended to be similar for all patient groups (Table 4).

Variations in regional activity retention between the 240-min and 30-min SPECT examination of the brain were evaluated by comparing the activity uptake ratio for the two imaging times in 24 regions of the brain. The mean uptake ratios for the different patient groups are shown in Table 5.

An estimate of regional ^{123}I-IMP uptake from the whole-body scans, in terms of percent retained dose, was calculated from the geometric means of conjugate paired ROIs over the brain, lungs and liver compared to the whole body. The results were as follows: (c-ns) brain = 5.8 ± 0.9, lungs = 15.0 ± 2.6, liver = 19.3 ± 3.2 (n = 13); (c-s) brain = 4.7 ± 1.2, lungs = 22.1 ± 6.9, liver = 16.6 ± 2.9 (n = 7);

TABLE 2
Iodine-123-IMP Cerebral Uptake (0–25 min)

	T_1* (sec)	T_2* (sec)	T_{50} (sec)	T_{90} (sec)	γ (c/37 MBq/100p)
Control (n = 21)	14 ± 5	340 ± 22	72 ± 47	806 ± 220	3.4 ± 1.5
Nonsmokers (14)	15 ± 5	345 ± 22	70 ± 40	801 ± 191	4.0 ± 1.4
Smokers (7)	12 ± 6	328 ± 50	77 ± 63	775 ± 283	2.3 ± 0.8
Crack (n = 21)	16 ± 6	419 ± 41	90 ± 60	1005 ± 92	3.1 ± 1.0
Nonsmokers (5)	13 ± 6	391 ± 35	101 ± 56	989 ± 99	3.3 ± 1.1
Smokers (16)	17 ± 6	432 ± 38	85 ± 62	1012 ± 92	3.1 ± 1.0
		p-values			
Controls (21) vs. crack (21)	—	0.001	—	0.0003	—
Controls					
Nonsmokers (14) vs. smokers (7)	—	—	—	—	0.009
Crack					
Nonsmokers (5) vs. smokers (16)	—	0.03	—	—	—
Nonsmokers					
Controls (14) vs. crack (5)	—	0.03	—	0.04	—
Smokers					
Controls (7) vs. crack (16)	—	0.009	—	0.007	—

*$y(t) = \gamma - \alpha_1 e^{-\lambda_1 t} - \alpha_2 e^{-\lambda_2 t}$, where $T_1 = \ln 2/\lambda_1$, $T_2 = \ln 2/\lambda_2$

(cr-ns) brain = 4.3 ± 0.6, lungs = 14.9 ± 2.1, liver = 21.6 ± 1.4 (n = 4); (cr-s) brain = 4.7 ± 1.0, lungs = 23.1 ± 6.6, liver = 16.3 ± 4.2 (n = 13).

DISCUSSION

Initial Uptake and Localization Properties

Cocaine use in the United States is widespread. Gawin and Ellinwood, Jr. estimated that in 1986, 3 to 5 million people in the U.S. used cocaine regularly and that 15% of the U.S. population had tried cocaine, including 40% of those between the ages of 25 and 30 years (*17*). Its use is widespread despite well-documented observations which show cocaine to be a dangerous reinforcing drug that is a potent vasoconstrictor and neurotransmitter blocking agent (*18*). Cocaine has been documented to cause many serious medical problems affecting metabolism and function in the heart, brain, lungs, muscle and other tissues (*7–9,17,18*). In the brain, cocaine use has been shown to lead to cerebral infarction, subarachnoid and intracerebral hemorrhage, cerebral ischemia, vascular spasm and cerebral vasculitis (*7–8*). Here we investigated the use of the brain SPECT imaging procedure to see if it could be used to detect alterations in rCBF in advance of overt clinical symptomatology.

TABLE 3
Iodine-123-IMP Uptake Ratios:
Perfusion Defect ROI-to-Contralateral ROI

Subject no.	Region	Slice no.	Uptake ratio: Perfusion defects	Uptake ratio: Control subjects
2	Frontal	4	0.82	1.04 ± 0.10
	Parieto-occipital	4	0.85	1.00 ± 0.06
12	Occipital	7	0.95	1.02 ± 0.04
16	Occipital	6	0.88	1.01 ± 0.03
3	Occipital	7	0.96	1.02 ± 0.04
9	Parietal	4	0.89	1.00 ± 0.04
	Temporal	6	0.84	0.99 ± 0.05
13	Occipital	6	0.94	1.01 ± 0.03

The results of this study suggest that ^{123}I-IMP SPECT brain imaging could offer a sensitive assay of alterations in regional brain perfusion in crack abuse. Measurements made to characterize the uptake rate of the radiopharmaceutical into the brain showed that the average biologic T_2 of ^{123}I-IMP uptake in the brain of crack users was 23% longer than in controls (Table 2). The findings suggest that a history of smoking may further alter uptake rate. Whereas significant differences in T_2 were seen between nonsmoking controls and smoking crack users, T_2 was 10% longer in smoking crack users than in nonsmoking crack users ($p = 0.03$), and T_2 was 32% longer in smoking crack users than in smoking controls ($p = 0.009$). A decrease of 43% in the average plateau activity level, γ, of smoking as compared with nonsmoking controls, suggests that smoking alters the amount of ^{123}I-IMP that reaches the brain. Furthermore, γ differences of <7% found between smoking and nonsmoking crack users, and γ decreases of 18%–23% found in smoking and nonsmoking crack users compared with nonsmoking controls, suggest that the effect of crack use on uptake in the brain is similar to that of cigarette smoke. The average retained dose in the brain of nonsmoking controls from the whole-body scans at 75–105 min was consistently higher (19%–26%) than in smoking controls, nonsmoking crack users and smoking crack users. In comparison, the average lung activity was consistently greater in smokers. Smoking control subjects on the average showed 47% more activity in the lungs on the

TABLE 4
Activity Ratio: Region-to-Cerebellum

Region	Slice no.	All		Nonsmokers(ns)		Smokers(s)	
		Control(c) n = 21	Crack(cr) n = 21	Control(c) n = 14	Crack(cr) n = 5	Control(c) n = 7	Crack(cr) n = 16
Prefrontal	3	1.03 ± 0.08	1.02 ± 0.07	1.03 ± 0.09	1.05 ± 0.06	1.04 ± 0.07	1.01 ± 0.08
	4	1.03 ± 0.10	1.04 ± 0.08	1.03 ± 0.12	1.07 ± 0.06	1.03 ± 0.06	1.03 ± 0.08
	6	1.01 ± 0.10	1.05 ± 0.09	1.01 ± 0.12	1.07 ± 0.08	1.00 ± 0.07	1.05 ± 0.09
	7	0.97 ± 0.10	1.01 ± 0.08	0.98 ± 0.12	1.04 ± 0.11	0.96 ± 0.06	1.00 ± 0.07
	8	0.67 ± 0.15	0.72 ± 0.15	0.69 ± 0.17	0.80 ± 0.16	0.63 ± 0.09	0.70 ± 0.14
	9	0.46 ± 0.09	0.47 ± 0.10	0.46 ± 0.011	0.48 ± 0.08	0.46 ± 0.05	0.46 ± 0.10
Frontal	3	0.97 ± 0.08	0.95 ± 0.06	0.97 ± 0.09	0.99 ± 0.07	0.98 ± 0.08	0.94 ± 0.05
	4	0.96 ± 0.08	0.93 ± 0.06	0.95 ± 0.09	0.96 ± 0.05	0.98 ± 0.09	0.93 ± 0.06
	6	0.92 ± 0.07	0.93 ± 0.07	0.91 ± 0.08	0.96 ± 0.06	0.93 ± 0.05	0.92 ± 0.07
	7	0.88 ± 0.09	0.88 ± 0.06	0.87 ± 0.09	0.92 ± 0.07	0.89 ± 0.07	0.87 ± 0.05
Parietal	3	0.97 ± 0.07	0.96 ± 0.06	0.97 ± 0.07	1.01 ± 0.05	0.98 ± 0.07	0.95 ± 0.06
	4	0.98 ± 0.06	0.94 ± 0.07	0.98 ± 0.05	0.95 ± 0.07	0.99 ± 0.09	0.94 ± 0.07
Temporal	6	1.02 ± 0.07	1.02 ± 0.07	1.02 ± 0.07	1.05 ± 0.10	1.01 ± 0.08	1.01 ± 0.06
	7	0.99 ± 0.07	1.02 ± 0.05	0.99 ± 0.07	1.03 ± 0.05	0.99 ± 0.06	1.02 ± 0.06
	8	0.84 ± 0.05*	0.91 ± 0.07*	0.86 ± 0.06†	0.94 ± 0.04†	0.80 ± 0.03*	0.91 ± 0.08*
	9	0.65 ± 0.11*	0.76 ± 0.10*	0.67 ± 0.12†	0.82 ± 0.07†	0.61 ± 0.06*	0.75 ± 0.11*
Thalamus	6	0.96 ± 0.10	0.91 ± 0.11	0.97 ± 0.09	0.99 ± 0.16	0.95 ± 0.06	0.96 ± 0.08
Basal ganglia	6	0.93 ± 0.08	0.91 ± 0.11	0.92 ± 0.08	0.92 ± 0.16	0.93 ± 0.08	0.91 ± 0.09
	7	0.96 ± 0.08	0.98 ± 0.08	0.96 ± 0.09	0.99 ± 0.09	0.95 ± 0.06	0.98 ± 0.08
Visual cortex	3	1.07 ± 0.08	1.04 ± 0.07	1.05 ± 0.07	1.11 ± 0.04	1.10 ± 0.08†	1.02 ± 0.06†
	4	1.10 ± 0.07†	1.05 ± 0.07†	1.10 ± 0.06	1.10 ± 0.06	1.11 ± 0.09†	1.04 ± 0.07†
	6	1.10 ± 0.07	1.06 ± 0.07	1.11 ± 0.06	1.09 ± 0.06	1.08 ± 0.09	1.05 ± 0.07
Cerebellum	8	1.00 ± 0.02	0.97 ± 0.05	1.00 ± 0.01	1.00 ± 0.05	1.00 ± 0.03	0.96 ± 0.04
	9	1.01 ± 0.04	0.99 ± 0.02	1.01 ± 0.04	0.98 ± 0.02	1.00 ± 0.05	1.00 ± 0.02

*$0.0009 \leq p \leq 0.004$.
†$0.01 \leq p \leq 0.05$.

whole-body scans than nonsmoking controls and smoking crack users showed 55% greater uptake than the nonsmoking crack users.

Recently, other investigators have shown that ^{123}I-IMP clearance from the lungs is delayed in cigarette smokers and that variations in lung uptake can influence the activity reaching the brain (*19–21*). The time-activity curve for ^{123}I-IMP clearance from the lung in these studies is characterized by a dual-exponential equation, where an initial fast component ($t_{1/2} \leq 3$ min) is thought to reflect the rapid clearance of the nonsaturable amines and the longer-lived component reflects the washout of the saturable amines with partitioning into different compartments. Alveolar macrophages bind the saturable amines and play a major role in their release. With macrophage activity enhanced and modified in smokers (*21*), it is not surprising to see alterations in clearance time. It is the change in this slower component that is suspected to be the cause of greater retention in the lungs in cigarette smokers. The decrease in activity available to the circulation probably reduces the activity which reaches the brain of cigarette smokers. Whether the decreases in the rate of cerebral uptake and the amount of ^{123}I-IMP activity reaching the brain of crack users only reflects the effects of smoking on the lungs, or may also include additional effects of cocaine on the brain, such as cocaine-blocked amine receptor sites, or is the result of other factors, could not be answered from the observations in our study.

SPECT

The high incidence of perfusion defects and loss of contrast and definition of gray matter structures seen on the early (30-min) SPECT images of the brain of crack users are consistent with decreased blood flow in the cortex and may reflect ischemic changes due to focal vasoconstriction, spasm or cerebral vasculitis resulting from crack abuse. Neurovascular changes are frequently cited in the literature on cocaine abuse (*7–9,23–29*). Figure 5 shows an example of a set of images interpreted as having severe mottled uptake with a grade of 4. Cortical borders are poorly defined with mottled uptake seen throughout the cortical, subcortical and cerebellar structures. The obser-

TABLE 5
Regional ^{123}I-IMP Retention:
4 hr-to-0.5 hr SPECT ROI Uptake Ratio

Region	Slice no.	All		Nonsmokers(ns)		Smokers(s)	
		Control(c) (n = 21)	Crack(cr) (n = 21)	Control(c) (n = 14)	Crack(cr) (n = 5)	Control(c) (n = 7)	Crack(cr) (n = 16)
Prefrontal	3	0.70 ± 0.10	0.67 ± 0.12	0.67 ± 0.10	0.65 ± 0.04	0.75 ± 0.11	0.68 ± 0.14
	4	0.70 ± 0.11	0.67 ± 0.14	0.67 ± 0.09	0.65 ± 0.07	0.77 ± 0.10	0.68 ± 0.15
	6	0.70 ± 0.09	0.67 ± 0.13	0.68 ± 0.09	0.66 ± 0.07	0.75 ± 0.08	0.67 ± 0.15
	7	0.71 ± 0.08	0.68 ± 0.14	0.68 ± 0.08	0.65 ± 0.10	0.76 ± 0.07	0.68 ± 0.16
	8	0.66 ± 0.11	0.60 ± 0.17	0.67 ± 0.10	0.53 ± 0.05	0.69 ± 0.14	0.63 ± 0.19
	9	0.65 ± 0.11	0.62 ± 0.15	0.65 ± 0.11	0.58 ± 0.09	0.66 ± 0.15	0.63 ± 0.16
Frontal	3	0.72 ± 0.10	0.71 ± 0.14	0.69 ± 0.09	0.69 ± 0.08	0.79 ± 0.10	0.72 ± 0.16
	4	0.73 ± 0.11	0.73 ± 0.15	0.70 ± 0.10	0.70 ± 0.07	0.78 ± 0.12	0.74 ± 0.17
	6	0.73 ± 0.11	0.73 ± 0.15	0.70 ± 0.11	0.68 ± 0.06	0.78 ± 0.10	0.74 ± 0.17
	7	0.71 ± 0.08	0.72 ± 0.16	0.68 ± 0.08	0.69 ± 0.10	0.77 ± 0.07	0.72 ± 0.18
Parietal	3	0.73 ± 0.11	0.71 ± 0.13	0.71 ± 0.12	0.69 ± 0.08	0.72 ± 0.14	0.78 ± 0.08
	4	0.72 ± 0.08	0.73 ± 0.14	0.69 ± 0.07	0.73 ± 0.10	0.77 ± 0.07	0.73 ± 0.16
Temporal	6	0.71 ± 0.08	0.69 ± 0.14	0.68 ± 0.07	0.66 ± 0.07	0.76 ± 0.07	0.70 ± 0.15
	7	0.72 ± 0.09	0.69 ± 0.13	0.69 ± 0.05	0.66 ± 0.04	0.77 ± 0.08	0.69 ± 0.15
	8	0.75 ± 0.08	0.72 ± 0.14	0.73 ± 0.07	0.69 ± 0.02	0.78 ± 0.09	0.73 ± 0.16
	9	0.74 ± 0.10	0.69 ± 0.17	0.72 ± 0.09*	0.62 ± 0.03*	0.77 ± 0.13	0.71 ± 0.19
Thalamus	6	0.73 ± 0.10	0.70 ± 0.15	0.68 ± 0.08	0.68 ± 0.08	0.70 ± 0.16	0.83 ± 0.05
Basal ganglia	6	0.76 ± 0.11	0.72 ± 0.15	0.72 ± 0.09	0.71 ± 0.05	0.85 ± 0.10	0.73 ± 0.17
	7	0.73 ± 0.11	0.68 ± 0.15	0.69 ± 0.10	0.69 ± 0.06	0.82 ± 0.10	0.68 ± 0.17
Visual cortex	3	0.67 ± 0.10	0.65 ± 0.13	0.65 ± 0.10	0.63 ± 0.06	0.72 ± 0.07	0.65 ± 0.15
	4	0.65 ± 0.09	0.64 ± 0.13	0.62 ± 0.07	0.62 ± 0.06	0.70 ± 0.09	0.65 ± 0.15
	6	0.62 ± 0.09	0.62 ± 0.13	0.59 ± 0.07	0.58 ± 0.07	0.69 ± 0.10	0.63 ± 0.14
Cerebellum	8	0.62 ± 0.08	0.63 ± 0.13	0.59 ± 0.07	0.61 ± 0.04	0.69 ± 0.08	0.63 ± 0.14
	9	0.63 ± 0.09	0.62 ± 0.13	0.59 ± 0.07	0.62 ± 0.04	0.71 ± 0.10	0.62 ± 0.15

*p = 0.02.

vations seen in crack users appear to reflect the high sensitivity of the rCBF SPECT procedure to detect alterations in perfusion before clinical symptomatology is expressed.

Alterations in rCBF images have been reported with PET imaging using ^{15}O-labeled water in intravenous cocaine or free base abuse without abnormalities on physical and neurological examinations (*12*). The study showed a high incidence of reduced activity throughout the brain except for the cerebellum, focal reduced activity in the anterior areas of the brain and "patchy" areas of tracer localization throughout the brain. The results are similar to the results reported here with the exception that focal defects were seen primarily in the prefrontal cortex. Our SPECT study shows focal defects to be more widespread, with defects seen in the occipital, parietal, temporal and frontal cortex (Table 3). These observations are in agreement with the other two studies of drug abuse that involve PET imaging with ^{18}F-FDG in cocaine users and SPECT imaging with ^{99m}Tc-HMPAO in polydrug users (*11,13*). An additional high incidence of perfusion abnormalities in the basal ganglia was also reported in the ^{99m}Tc-HMPAO SPECT study. It is proposed that these findings are not the result of differences in the localization properties of the two radiopharmaceuticals or differences in rCBF between polydrug and crack users, but probably reflect the higher spatial resolution properties of the dedicated SPECT imaging system used in that investigation.

No focal perfusion defects were observed in SPECT studies of 21 control subjects. Fifteen of 21 subjects were read as normal and 6/21 subjects were interpreted as showing abnormally irregular and variable uptake throughout the cortex and loss of definition in cortical structures. In the last group, five of six subjects had small to moderate changes (grade 1 or 2) and one of six showed highly irregular uptake with the cortex of the right hemisphere poorly visualized. With four of six of the controls who were also smokers showing abnormal uptake, these findings are felt to reflect, in part, the loss in image quality associated with reduced activity reaching the brain in cigarette smokers. The higher sensitivity of dedicated multiple detector or ring type SPECT systems with similar or better spatial resolution would aid in the workup of these subjects to discrim-

inate focal perfusion defects from loss in definition of cortical structures resulting from limited photon statistics.

Delayed images at 240 min in all subjects indicated a tendency towards loss in contrast and sharp borders between gray and white matter structures, suggesting slow but progressive changes towards equilibration of activity in the gray and white matter of the brain. A potentially significant observation in the crack users was the complete or partial filling in of the perfusion defects on the 240-min SPECT study. Based on some work reported with rCBF imaging in cerebrovascular disease (*30*), it is possible that this filling in of hypoperfused regions on delayed images indicates regions of ischemia that retain a patent, but limited, blood supply.

No significant correlation was found between the incidence or degree of abnormal findings (Table 3) and length of time of crack use (<5 yr, n = 11 compared to >5 yr, n = 10), the amount of crack use per week (<10 g/wk, n = 11 compared to >10 g/wk, n = 10) or age (20–30 yr, n = 10 compared to 31–50 yr, n = 11). The uncertainty in the reliability of the patient's history to accurately document drug use may be a factor in this finding. A similar lack of correlation, however, was seen in the earlier referenced SPECT study which involved polydrug users and in the PET study which included both intravenous injection and freebase cocaine users (*11,12*).

The quantitative workup of the regional uptake properties of ^{123}I-IMP seen in brain SPECT involved evaluation of: (1) contralateral activity uptake ratios of paired regions of the cerebral cortex, basal ganglia, thalamus and cerebellum; (2) a comparison of all ROIs to cerebellum for the 30-min SPECT images; and (3) a comparison of each ROI to itself between the 240-min and 30-min SPECT procedures (Tables 4–5). The mean contralateral uptake ratios and the ratios of regions to the cerebellum showed no significant quantitative differences ($p > 0.05$) in uptake between control and crack users when treated as two groups or when divided into smokers and nonsmokers. Differences in the cerebellar uptake ratios for the different groups of subjects were ≤10%, with exception of differences on the order of 9%–23% observed in two of four of the most distal regions of the temporal lobe. With adequate region selection being highly dependent on the horizontal positioning of the brain in the transverse presentation, these were felt to reflect errors in ROI placement rather than significant differences in temporal lobe uptake.

The ratios of the counts (activity) in the 240-min to 30-min ROIs were used to evaluate the differences in regional tracer clearance due to redistribution or removal. Table 5 summarizes these data. It shows that only two regions, one of the five ROIs in the prefrontal cortex from slice 8 and one of three ROIs in the temporal cortex from slice 9, out of 24 show significant differences in regional ^{123}I-IMP uptake. These were considered insignificant since the remaining ROIs over both regions showed no significant differences between the crack user and the control groups.

The small and limited number of changes observed between the average uptake ratios in controls and crack users reflect the small changes in uptake that occur in areas of decreased blood flow with crack abuse. Focal perfusion defects observed on SPECT showed 4%–16% less uptake than the contralateral or adjacent control region (Table 3). Quantifying the activity ratios between groups of crack users and controls characterizes the range of activity gradients seen in perfusion defects in this population.

In summary, the results indicate that significant alterations in cerebral perfusion occur in a high percentage of asymptomatic crack users. Quantitative indices developed from ^{123}I-IMP SPECT and associated imaging procedures show that the rate of uptake, the amount and the localization properties of ^{123}I-IMP provide a sensitive and efficient means of investigating the effects of crack abuse on cerebral perfusion.

ACKNOWLEDGMENT

Research supported by U.S. DOE contract DE-AC02-76CH00016.

REFERENCES

1. Weber DA, Devous MD, Tikofsky RS, Woodhead AD, Vivirito KJ, eds. *Brain SPECT perfusion imaging: image acquisition, processing, display, and interpretation.* DOE CONF-91103668, 1992:1–132.
2. Baldwin RM. Iofetamine HCl ^{123}I(IMP). In: Weber DA, Devous MD, Tikofsky RS, Woodhead AD, Vivirito KJ, eds. *Brain SPECT perfusion imaging: image acquisition, processing, display, and interpretation.* DOE CONF-91103668, 1992:1–6.
3. Kuhl DE, Barrio JR, Huang, et al. Quantifying local cerebral blood flow by N-isopropyl-p-[^{123}I] iodoamphetamine (IMP) tomography. *J Nucl Med* 1982;23:196–203.
4. Lassen NA, Henriksen L, Holm S, et al. Cerebral blood-flow tomography: xenon-123 compared with isopropyl-amphetamine-iodine-123: concise communication. *J Nucl Med* 1983;24:17–21.
5. Devous MD, Stokely EM, Chehabi HH, Bonte FJ. Normal distribution of regional cerebral blood flow measured by dynamic single-photon emission tomography. *J Cereb Blood Flow Metab* 1986;6:95–104.
6. Susskind H, Weber DA. Effect of cocaine on the distribution of I-123-IMP in the dog's brain and lungs [Abstract]. *J Nucl Med* 1990;31:887.
7. Jacobs IG, Rosler MH, Kelly JK, Klein MA, Kling GA. Cocaine abuse: neurovascular complications. *Radiology* 1989;170:223–227.
8. Brown E, Prager J, Lee H-Y, Ramsey RG. CNS complications of cocaine abuse: prevalence, pathophysiology, and neuroradiology. *Am J Roentgenol* 1992;159:137–147.
9. Levine SR, Brust JCM, Futrell N, et al. Cerebrovascular complications of the use of "crack" form of alkaloidal cocaine. *N Engl J Med* 1990;323:699–704.
10. Tumeh SS, Nagel JS, English RJ, Moore M, Holman BL. Cerebral abnormalities in cocaine abusers: demonstration by SPECT perfusion brain scintigraphy. *Radiology* 1990;176:821–824.
11. Holman LJ, Carvahlo PA, Mendelson J, et al. Brain perfusion is abnormal in cocaine-dependent polydrug users: a study using technetium-99m-HMPAO and ASPECT. *J Nucl Med* 1991;32:1206–1210.
12. Volkow ND, Mullani N, Gould KL, Adler S, Krajewski K. Cerebral blood flow in chronic cocaine users: a study with positron emission tomography. *Br J Psychiatry* 1988;152:641–648.
13. Baxter LR, Jr, Schwartz JM, Phelps ME, et al. Localization of neurochemical effects of cocaine and other stimulants in the human brain. *J Clin Psychiatry* 1988;49:23–26.
14. Pohl P, Vogl G, Fill H, Rossler H, Zangerle R, Gerstenbrand F. Single-photon emission computed tomography in AIDS dementia complex. *J Nucl Med* 1988;29:1382–1386.
15. Chang LT. A method for attenuation correction in radionuclide computed tomography. *IEEE Trans Nucl Sci* 1978;NS 25:638–643.
16. Weber DA, Ivanovic I, Cabahug C, Sacker DF, Wong CTC. Experimental

approach to attenuation coefficient and filter selection in brain SPECT. *Eur J Nucl Med* 1991;18:669.
17. Gawin FH, Ellinwood EH Jr. Cocaine and other stimulants. *N Engl J Med* 1988;318:1173–1183.
18. Gregler LL, Mark H. Medical complications of cocaine abuse. Special report. *N Eng J Med* 1986;315:1495–1500.
19. Yonekura Y, Fujita T, Nishizawa S, Iwasaki Y, Mukai T, Konishi J. Temporal changes in accumulation of N-isopropyl-p-iodoamphetamine in human brain: relation to lung clearance. *J Nucl Med* 1989;30:1977–1981.
20. Ikeda H, Mariko M, Komatsu M, Takahashi K, Yasui S, Takahashi K. Prolonged lung retention of ^{123}I-IMP in pulmonary disease. *Eur J Nucl Med* 1989;15:646–648.
21. Kato K, Harada S, Takahashi T, Latsuragawa S, Yanagisawa T. Effects of cigarette smoking on iodine-123-N-isopropyl-p-iodoamphetamine clearance from the lung. *J Nucl Med* 1991;18:801–805.
22. Iijima N, Sato T, Yamamoto M, et al. Morphometry of human alveolar macrophage in smokers and non-smokers [Abstract]. *Am Rev Respir Dis* 1991;141:A338.
23. Isner JM, Chokshi SK. Cocaine and vasospasm. *N Engl J Med* 1989;23: 1604–1606.
24. Riggs D, Weibley RE. Acute toxicity from oral ingestion of crack cocaine: a report of four cases. *Pediatric Emergency Care* 1990;6:24–26.
25. Golbe LI, Merkin MD. Cerebral infarction in a user of free-base cocaine ("crack"). *Neurology* 1986;36:1602–1604.
26. Kaye BR, Fainstat M. Cerebral vasculitis associated with cocaine abuse. *JAMA* 1987;15:2104–2106.
27. Krendel DA, Ditter SM, Frankel MR, Ross WK. Biopsy-proven cerebral vasculitis associated with cocaine abuse. *Neurology* 1990;40:1092–1094.
28. Lowenstein DH, Massa SM, Rowbotham MC, Collins SD, McKinney HE, Simon RP. Acute neurologic and psychiatric complications associated with cocaine abuse. *Am J Med* 1987;83:841–846.
29. Mody CK, Miller BL, McIntyre HB, Cobb SK, Goldberg MA. Neurologic complications of cocaine abuse. *Neurology* 1988;38:1189–1193.
30. Ksukuda M, Kuwabara Y, Ichiya Y, et al. Evaluation of the significance of "redistribution" in I-123 IMP SPECT in cerebrovascular disorders—a comparative study with PET. *Eur J Nucl Med* 1989;15:746–749.

SELF-STUDY TEST

Skeletal Nuclear Medicine

Questions are taken from the *Nuclear Medicine Self-Study Program 1,* published by The Society of Nuclear Medicine

DIRECTIONS

Items 1-10 consist of five lettered headings followed by a list of numbered phrases or statements. For each numbered phrase or statement, select the one lettered heading that is most closely associated with it. Each lettered heading may be selected once, more than once, or not at all. Answers may be found on page 952.

For each bone-seeking agent (items 1-4), select the moiety (options A-E) for which it substitutes in the hydroxyapatite crystal.

A. Calcium
B. Phosphate
C. Magnesium
D. Hydroxyl
E. Sulfhydryl

1. ^{99m}Tc diphosphonate
2. ^{18}F fluoride
3. ^{99m}Tc pyrophosphate
4. ^{87m}Sr

For each of the ^{99m}Tc MDP images shown in Figures 1, 2 and 3 (items 5-7), select the most likely mechanism for the nonosseous localization of the radiopharmaceutical (options A-E).

A. Excessive free reduced ^{99m}Tc in the radiopharmaceutical, with colloid formation
B. Metastatic calcification
C. Heterotopic ossification
D. Dystrophic calcification
E. Increased local concentration of tracer

5. Figure 1
6. Figure 2
7. Figure 3

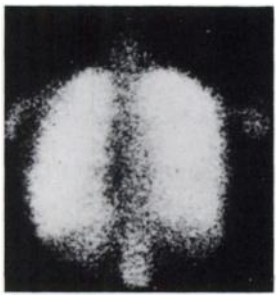

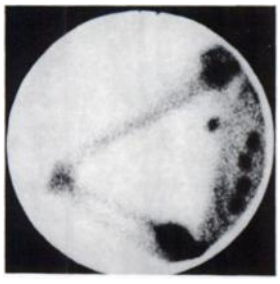

Figure 1

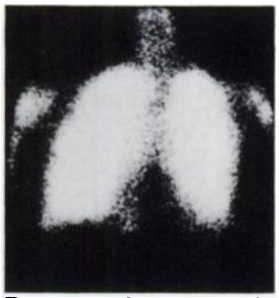

Figure 2

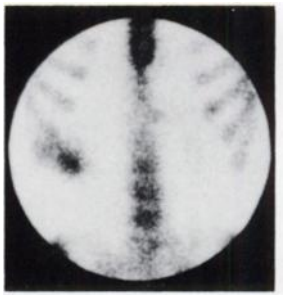

Figure 3

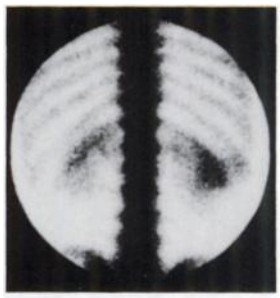

(continued on page 952)